Gravitational-Wave Extraction from an Inspiraling Configuration of Merging Black Holes

John G. Baker,[1] Joan Centrella,[1] Dae-Il Choi,[1,2] Michael Koppitz,[1] and James van Meter[1]

[1]*Gravitational Astrophysics Laboratory, NASA Goddard Space Flight Center, 8800 Greenbelt Road, Greenbelt, Maryland 20771, USA*

[2]*Universities Space Research Association, 10211 Wincopin Circle, Suite 500, Columbia, Maryland 21044, USA*

(Received 15 November 2005; published 22 March 2006)

We present new ideas for evolving black holes through a computational grid without excision, which enable accurate and stable evolutions of binary black hole systems with the accurate determination of gravitational waveforms directly from the wave zone region. Rather than excising the black hole interiors, our approach follows the ''puncture'' treatment of black holes, but utilizing a new gauge condition which allows the black holes to move successfully through the computational domain. We apply these techniques to an inspiraling binary, modeling the radiation generated during the final plunge and ringdown. We demonstrate convergence of the waveforms and good conservation of mass-energy, with just over 3% of the system's mass converted to gravitational radiation.

DOI: 10.1103/PhysRevLett.96.111102 PACS numbers: 04.25.Dm, 04.30.Db, 04.70.Bw, 95.30.Sf

Coalescing comparable mass black hole binaries are prodigious sources of gravitational waves. The final merger of these systems will produce an intense burst of gravitational radiation and is expected to be among the strongest sources for ground-based gravitational-wave detectors, which will observe the mergers of stellar-mass and intermediate-mass black hole binaries, and the space-based Laser Interferometer Space Antenna (LISA), which will detect mergers of massive black hole binaries. With the first-generation Laser Interferometer Gravitational-Wave Observatory now in a year-long science data-taking run and LISA moving forward through the formulation phase, the need for accurate merger waveforms has become urgent.

Such waveforms can be obtained only through 3D numerical relativity simulations of the full Einstein equations. While this has proven to be a very challenging undertaking, new developments allow an optimistic outlook. Full 3D evolutions of binary black holes, in which regions within the horizons have been excised from the computational grid, have recently been carried out. Using corotating coordinates, so that the holes remain fixed on the grid as the system evolves, a binary has been evolved through a little more than a full orbit [1] as well as through a plunge, merger, and ringdown [2], though without being able to extract gravitational waveforms. More recently, a simulation in which excised black holes (arising from the collapse of an unstable scalar field configuration) move through the grid in a single plunge orbit, merger, and ringdown has been accomplished, with the calculation of a waveform [3].

In this Letter, we present new ideas which allow the black holes to move through the coordinate grid without the need for excision [4]. We also report the results of new simulations of inspiraling binary black holes through merger and ringdown, carried out using these new techniques. With fixed mesh refinement, we are able to resolve both the dynamical region where the black holes inspiral (with length scales $\sim M$, where M is the total system mass, and we set $c = G = 1$) and the outer regions where the gravitational waves propagate [length scales $\sim(10\text{–}100)M$]. Using an outer boundary at $128M$, we evolve the system stably to well beyond $t \approx 100M$, extract gravitational waveforms, and demonstrate that they are 2nd-order convergent.

We start by setting up data for equal mass binary black holes represented as ''punctures'' [5]. The metric on the initial spacelike slice takes the form $g_{ij} = \psi^4 \delta_{ij}$, where $i, j = 1, 2, 3$, and the conformal factor $\psi = \psi_{\mathrm{BL}} + u$. The static, singular part of the conformal factor has the form $\psi_{\mathrm{BL}} = 1 + \sum_{n=1}^{2} m_n/2|\vec{r} - \vec{r}_n|$, where the nth black hole has mass m_n and is located at $\vec{r}_n$. The nonsingular function u is obtained by solving the Hamiltonian constraint equation using AMRMG [6]. We use parameters so that the black holes have proper separation $4.99M$, and the system has total mass $M = 1.008$ and angular momentum $J = 0.779M^2$. This corresponds to the run QC0 studied in Ref. [7].

In the traditional puncture implementation, ψ_{BL} is factored out and handled analytically; only the regular parts of the metric are evolved. In this case, the punctures remain fixed on the grid while the binary evolves. However, the stretching of the coordinate system that ensues is problematic. First, as the physical distance between the black holes shrinks, certain components of the metric must approach zero, causing other quantities to grow uncontrollably. Second, a corotating coordinate frame (implemented by an appropriate angular shift vector) is necessary to keep the orbiting punctures fixed on the grid; this causes extremely superluminal coordinate speeds at large distances from the black holes and, in the case of a Cartesian grid, incoming noise from the outer boundary.

Our approach is to allow the punctures to move freely through the grid, by not factoring out the singular part of the conformal factor but rather evolving it inseparably from the regular part. Initially, we follow the standard

puncture technique and set up the binary so that the centers of the black holes are not located at a grid point. Taking numerical derivatives of $\psi_{\rm BL}$ effectively regularizes the puncture singularity using the smoothing inherent in the finite differences. These regularized data are then evolved numerically. Since the centers of the black holes remain in the $z = 0$ plane, they do not pass through grid points in our cell-centered implementation.

We evolve this data with the HAHNDOL code, which uses a relatively standard conformal formulation of Einstein's evolution equations on a cell-centered numerical grid [8] with a box-in-box resolution structure implemented via PARAMESH [9]. The innermost refinement region is a cube stretching from $-2M$ to $2M$ in all three dimensions and has the finest resolution h_f. The punctures are placed within this region on the y axis in the $z = 0$ plane; we impose equatorial symmetry throughout. We performed three simulations with identical grid structures but with uniformly differing resolutions. In the most refined cubical region, the resolutions were $h_f = M/16$, $M/24$, and $M/32$. Subsequent boxes of doubled size have half the resolution; we use 8 boxes in all. Outgoing wave boundary conditions are applied at the outer boundary, which is located at $128M$ and causally disconnected from the wave extraction region through most of the run. We use 4th-order finite differencing for the spatial derivatives except for the advection of the shift, which is performed with 2nd-order, mesh-adapted differencing [10], and we use 2nd-order time stepping via a three-step iterative Crank-Nicholson scheme. The highest resolution run ran for $\sim$40 hours on 256 processors of an SGI Altix 3000 machine.

In our new approach, the free evolution of punctures is made possible by a modified version of a common coordinate condition known as the Gamma-freezing shift vector, which drives the coordinates towards quiescence as the merged remnant black hole also becomes physically quiescent. Our modified version retains this "freezing" property yet is suitable for motile punctures. Specifically, we use $\partial_t \beta^i = \frac{3}{4}\alpha B^i$ and $\partial_t B^i = \partial_t \tilde{\Gamma}^i - \beta^j \partial_j \tilde{\Gamma}^i - \eta B^i$, which incorporates two critical changes to the standard Gamma-freezing condition. A factor $\psi_{\rm BL}$ of the conformal factor, originally used to ensure that the shift vanishes at the puncture, has been removed in order to allow the punctures to move. Also, a new term has been added $(-\beta^j \partial_j \tilde{\Gamma}^i)$, which facilitates more stable and accurate evolution of moving punctures by eliminating a zero-speed mode (which was otherwise found to create a "puncture memory" effect as errors grew in place [11]). Along with this shift condition, we use the standard singularity-avoiding, 1 + log slicing condition on the lapse.

Figure 1 shows the error in the Hamiltonian constraint C_H at two different times. The peak violation near the puntures does not leak out, or grow with time, but stays well-confined even though the punctures and horizons move across the grid. Overall, we get 2nd-order convergence away from the horizons to well beyond the wave extraction region for the entire course of the run. There is no indication of exponentially growing constraint violations, which have plagued many numerical simulations with black holes fixed in place on the numerical grid.

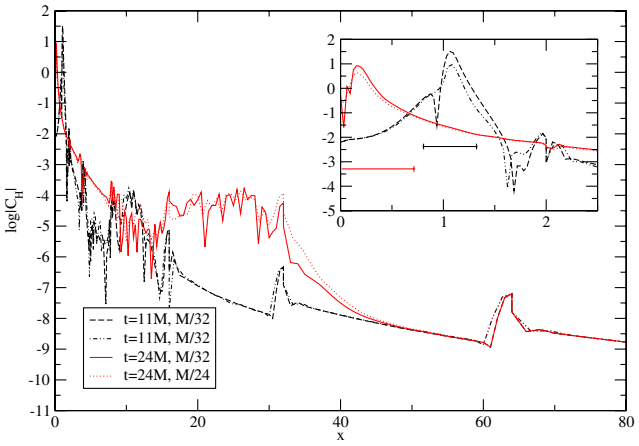

FIG. 1 (color online). Hamiltonian constraint error C_H at two times, $t = 11M$ and $t = 24M$, when a puncture is near to crossing the positive x axis. Two resolutions are shown, $h_f = M/24$ and $M/32$, and the data are scaled such that the lines representing the different resolutions should superpose in the case of perfect 2nd-order convergence. The inset shows that C_H is well-behaved in the region near the punctures. The horizontal lines indicate the approximate location of the apparent horizons; at the later time, a common horizon has formed.

One way to get a picture of the motion of the black holes is to look at the location of the black hole apparent horizons at different times. Figure 2 shows the locations of a sequence of apparent horizons (calculated using the AHFINDERDIRECT code [12]) where they cross the x-y plane for our $h_f = M/16$ run. In the coordinates of our simulation, the black holes undergo about one-half orbit before forming a common horizon.

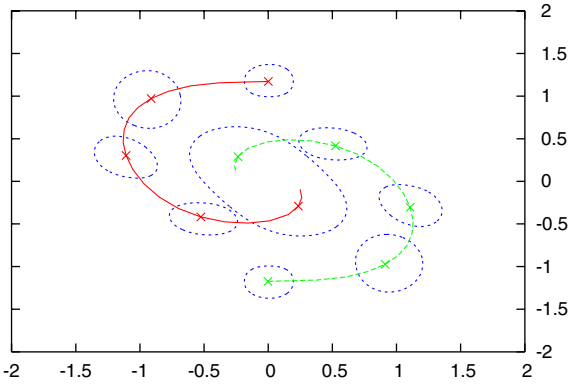

FIG. 2 (color online). The positions of the apparent horizons at times $t = 0$, 5, 10, 15, and $20M$ for our $M/16$ run. The curve shows the trajectories of centroids of the individual apparent horizons.

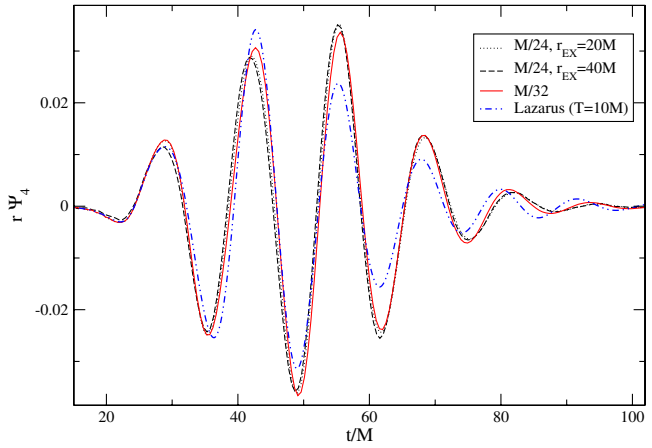

FIG. 3 (color online). Real part of $r\Psi_4$ extracted from the numerical simulation on spheres of radii $r_{\rm EX} = 20M$ and $40M$ for the medium and high resolution runs. The waveforms extracted at different radii have been rescaled by $1/r_{\rm EX}$ and shifted in time to account for the wave propagation time between the extraction spheres. At high resolution ($h_f = M/32$), there is no discernible dependence on extraction radius. For comparison, we show Lazarus waveforms from Ref. [7].

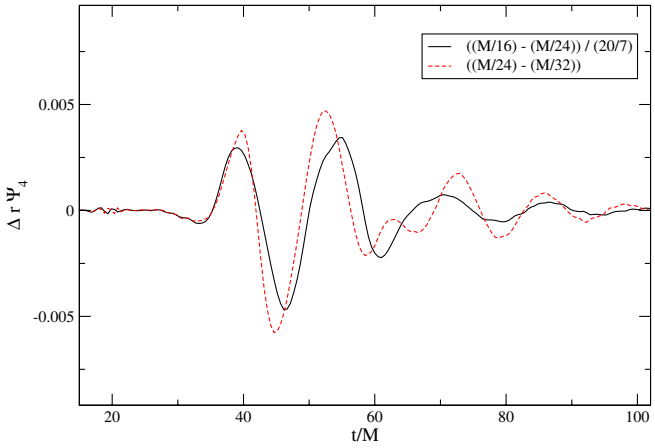

FIG. 4 (color online). Differences of the real part of $r\Psi_4$ for resolutions of $h_f = M/16$, $M/24$, and $M/32$ appropriately scaled such that, for perfect 2nd-order convergence, the lines would lay on top of each other.

We extract the gravitational waves generated by the merger using the technique explained in detail in Ref. [13]. Figure 3 shows the dominant $l = 2$, $m = 2$ components of the Weyl curvature scalar Ψ_4 extracted at two different radii from the medium and high resolution runs. For each resolution, the time-shifted and rescaled waveforms computed at different extraction radii are nearly indistinguishable, indicating that the waves travel cleanly across refinement boundaries and have the expected $1/r$ falloff. In addition, the two highest resolution waveforms differ only by a slight phase shift and a by few percent in amplitude. For comparison, we have also included the QC0 Lazarus waveforms from Sec. V of Ref. [7]. These were extracted by approximately matching the later portion of brief numerical simulations onto a perturbed black hole [14,15] at transition time $10M$.

Figure 4 shows the convergence of the extracted waves throughout the run. The difference between the two highest resolutions is roughly 90° out of phase with the waveform, corresponding to a small phase shift in the waveform, possibly caused by a small difference in the orbital trajectories.

The gravitational waveforms also contain physical information about the radiation, including the energy E and angular momentum J carried away by the radiation. We calculate dE/dt and dJ/dt from time integrals of all $l = 2$ waveform components using Eqs. (5.1) and (5.2) in Ref. [7]. Integrating dE/dt gives the energy loss as a function of time; this should be the same as $M - M_{\rm ADM}$, where $M_{\rm ADM}$ is the Arnowitt-Deser-Misner (ADM) mass extracted on a sphere of sufficiently large radius [16]. Figure 5 shows a comparison between $M - E$ and an independent calculation of $M_{\rm ADM}$ at two extraction radii $r_{\rm EX} = 40$ and $50M$. The striking consistency between the two calculations as the radiation passes indicates good energy conservation in the simulation. Shortly before the arrival of the radiation, the ADM mass measurement is affected by a transient nonphysical pulse in the gauge evolution, though the pulse does not affect the radiation measurement.

The total radiated energy calculated from the waveforms extracted at $r_{\rm EX} = 20$, 30, 40, and $50M$ in the highest resolution run has the values $E/M = 0.0304$, 0.0312, 0.0317, and 0.0319, respectively. While these values vary significantly with $r_{\rm EX}$ (even extracting at these relatively large radii), they are neatly consistent with a $1/r_{\rm EX}$ falloff

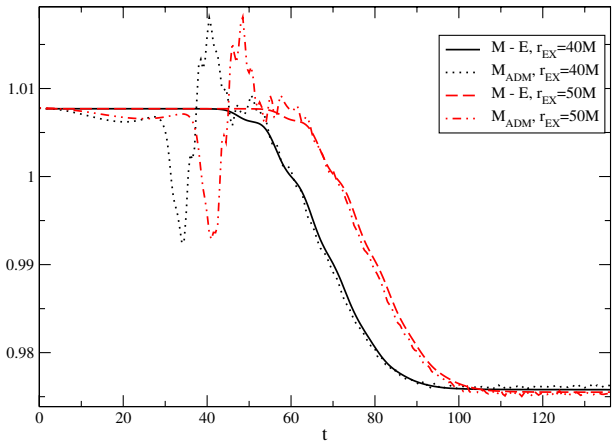

FIG. 5 (color online). Conservation of mass-energy for the highest resolution case, $h_f = M/32$. We compare the ADM mass $M_{\rm ADM}$ with the mass remaining $M - E$, after gravitational radiation energy loss E. The good agreement, based on extraction spheres at $r_{\rm EX} = 40$ and $50M$, indicates conservation of energy in the simulation.

TABLE I. The radiated energy E and angular momentum J carried away by gravitational radiation in our simulations.

	$M/16$	$M/24$	$M/32$	Lazarus	AEI
E/M	0.0516	0.0342	0.0330	0.025	0.030
J/M^2	0.208	0.140	0.138	0.10	0.17

to an asymptotic value of 0.0330 with an uncertainty in the extrapolation of $<1\%$. In Table I, we give the total radiated energies and angular momenta extrapolated as $r_{\mathrm{EX}} \rightarrow \infty$.

For comparison, we also include the Lazarus values, as well as values from the Albert Einstein Institute (AEI) group [2], which did not determine waveforms but estimated the radiative losses based on the state of the final black hole horizon in runs including the QC0 case. Our lowest resolution run clearly overestimates the radiation energy and angular momentum, while our higher resolution results are in closer agreement with the AEI value for the energy and close to the 20% level of confidence suggested in Ref. [7].

In conclusion, we present new ideas which allow puncture black holes to move through a grid without excision. Using a new gauge condition, we evolve an equal mass binary accurately and stably, from the initial inspiral orbit through merger and ringdown, and calculate the gravitational radiation waveform directly. The simulations converge with increasing resolution to 2nd order, leading to a 2nd-order convergence of the waveform. These waveforms have the correct $1/r$ falloff and agree to a great extent with approximately calculated ones. Our simulations show good energy conservation as indicated by comparing the change in ADM mass with the radiated energy. In this brief burst of gravitational radiation, we find that just over 3% of the system's initial mass-energy is carried away in gravitational waves.

This new gauge allows simulations to remain accurate far longer than previous standard puncture techniques. Since these new ideas have been developed within an overall numerical approach that is closely related to widely used numerical relativity techniques, they can be readily adopted by other groups using codes based on traditional conformal formulations of the Einstein equations. We plan to apply these techniques, using adaptive mesh refinement, to study binaries beginning from larger initial separation and different black hole initial configurations, which are expected to provide more realistic models corresponding to astrophysical systems. We will also study the effects of unequal black hole masses and the individual black hole spins.

We thank David Brown for providing AMRMG and Jonathan Thornburg for providing AHFINDERDIRECT, which we utilized with the assistance of Peter Diener and Thomas Radke. This work was supported in part by NASA Grant No. ATP02-0043-0056. The simulations were carried out using Project Columbia at NASA Ames Research Center and at the NASA Center for Computational Sciences at Goddard Space Flight Center. M. K. and J. v. M. were supported by the National Research Council.

[1] B. Bruegmann, W. Tichy, and N. Jansen, Phys. Rev. Lett. **92**, 211101 (2004).
[2] M. Alcubierre *et al.*, Phys. Rev. D **72**, 044004 (2005).
[3] F. Pretorius, Phys. Rev. Lett. **95**, 121101 (2005).
[4] While this Letter was being written, we learned that Campanelli and collaborators had independently developed similar techniques for moving black holes without excision, when both groups presented their results at the Numerical Relativity 2005 workshop (http://astrogravs.nasa.gov/conf/numrel2005/presentations/) on Nov. 2, 2005. Since then, Campanelli *et al.* have submitted a manuscript describing their work to the physics archive [17].
[5] S. Brandt and B. Brügmann, Phys. Rev. Lett. **78**, 3606 (1997).
[6] J. D. Brown and L. L. Lowe, J. Comput. Phys. **209**, 582 (2005).
[7] J. Baker, M. Campanelli, C. O. Lousto, and R. Takahashi, Phys. Rev. D **65**, 124012 (2002).
[8] B. Imbiriba *et al.*, Phys. Rev. D **70**, 124025 (2004).
[9] P. MacNeice, K. M. Olson, C. Mobarry, R. deFainchtein, and C. Packer, Comput. Phys. Commun. **126**, 330 (2000).
[10] J. G. Baker and J. R. van Meter, Phys. Rev. D **72**, 104010 (2005).
[11] J. G. Baker, J. M. Centrella, D.-I. Choi, and J. R. van Meter (to be published).
[12] J. Thornburg, Classical Quantum Gravity **21**, 743 (2004).
[13] D. R. Fiske, J. G. Baker, J. R. van Meter, D.-I. Choi, and J. M. Centrella, Phys. Rev. D **71**, 104036 (2005).
[14] J. Baker, B. Brügmann, M. Campanelli, C. O. Lousto, and R. Takahashi, Phys. Rev. Lett. **87**, 121103 (2001).
[15] J. Baker, M. Campanelli, and C. O. Lousto, Phys. Rev. D **65**, 044001 (2002).
[16] R. Arnowitt, S. Deser, and C. W. Misner, in *Gravitation: An Introduction to Current Research*, edited by L. Witten (Wiley, New York, 1962), pp. 227–265.
[17] M. Campanelli, C. O. Lousto, P. Marronetti, and Y. Zlochower, gr-qc/0511048.